



Diffusion of HTO, ^{36}Cl and ^{22}Na in the Mesozoic rocks of Northern Switzerland: III. Cross-lab comparison of diffusion measurements on argillaceous twin samples

Liesbeth Van Laer^{a,*}, Marc Aertsens^a, Norbert Maes^a, Luc R. Van Loon^b, Martin A. Glaus^b, Raphael A.J. Wüst^{c,d}

^a SCK-CEN, Belgian Nuclear Research Centre, Boeretang 200, 2400, Mol, Belgium

^b Paul Scherrer Institut, Forschungsstrasse 111, 5232, Villigen PSI, Switzerland

^c National Cooperative for the Disposal of Radioactive Waste – Nagra, Hardstrasse 73, 5430, Wettingen, Switzerland

^d Earth and Environmental Science, James Cook University, 4811, Townsville, Australia

ARTICLE INFO

Editorial handling by: Adrian Bath

Keywords:

Cross-lab

Benchmark study

Through-diffusion

Opalinus Clay

Clay rock

ABSTRACT

In the past decades, there has been a high interest in evaluations of argillaceous rock formations to host repositories for spent fuel or radioactive waste material. One of the main reasons for this interest is that argillaceous rocks are dominated by clay minerals, resulting in a fine-grained sediment matrix with micropores, low pore connectivity and thus low permeability, and good self-sealing properties. This entails that diffusion is the prime mechanism for transport of gas, fission products and radionuclides in clay-rich rocks. The determination of diffusion parameters is therefore key to evaluate the quality of the rock from long-term safety perspectives. Cross-lab comparison of diffusion data is however often challenging as various methods, concepts and models are utilised in the different laboratories across the globe. Here, a direct cross-lab comparison study of through-diffusion experiments was performed to compare and assess the effect of experimental method (through-diffusion) and modelling uncertainties of the parameters by comparing results obtained by two independent laboratories. The R&D group ‘Disposal’ at SCK CEN (Belgium) and the PSI-LES group (Switzerland) both performed through-diffusion experiments on (nearly) the same sample material using their in-house experimental and modelling methodologies for through-diffusion experiments. Adjacent (twin) samples at five depths between 870 and 940 m in the Trüllikon1-1 borehole (Switzerland) were selected and each lab subjected these five clay rock samples to diffusion in synthetic pore water with three different tracers, HTO, $^{36}\text{Cl}^-$ and $^{22}\text{Na}^+$, representative for neutral, anionic and cationic transport behaviour. The two labs used a similar design of diffusion cell and worked with similar experimental conditions, but there were small differences in the experimental set-up/conditions and in the modelling approach. The independently determined diffusion parameters from SCK CEN and PSI-LES for all three tracers confirmed previously observed uncertainties. For all three radionuclides, the variability of the effective diffusion coefficients estimated independently by both institutes was less than a factor 2 and in general much lower (deviations ranging between 0 and 73%). Besides, the parameter estimations of the capacity factor (or accessible porosity in case of HTO and $^{36}\text{Cl}^-$) agreed well. Moreover, the experimental datasets of HTO and $^{36}\text{Cl}^-$ were also cross-fitted. The evaluation revealed that the minor deviations can be attributed predominantly to variations in temperature (experimental conditions) and to a lesser extent to minor distinctions in the modelling approach. It is important to acknowledge that local heterogeneity might also contribute to these differences.

1. Introduction

Nuclear waste repositories in deep geological formations aim to

safely dispose spent fuel and radioactive waste for a long time (>1Ma) because of the presence of long-lived radionuclides. Representative and trustworthy data are critical for the evaluation of long-term safety and

* Corresponding author.

E-mail address: liesbeth.van.laer@sckcen.be (L. Van Laer).

<https://doi.org/10.1016/j.apgeochem.2023.105840>

Received 1 March 2023; Received in revised form 30 June 2023; Accepted 8 November 2023

Available online 25 November 2023

0883-2927/© 2024 The Authors. Published by Elsevier Ltd. This is an open access article under the CC BY license (<http://creativecommons.org/licenses/by/4.0/>).

performance of these systems and their components (NEA, 2013). Datasets used in these evaluations must be reliable, auditable and transparent. One of the most critical factors is the quantification of the transport rates of radionuclides through the host rock and their potential releases to the biosphere and thus its confinement performance. Clay-rich rocks have a fundamental retentive behaviour for radionuclides and their isolation from the biosphere is crucial to ensure long-term safety of waste material in such repositories. Since transport in clay-rich host rocks is dominated by diffusion, the determination of diffusion parameters is paramount and forms the basis for long-term safety and performance assessments.

Although different types of radionuclide migration experiments exist to study the transport behaviour of radionuclides in clay-rich rocks for the assessment of the geological formations as potential host rocks for the deep disposal of high-level radioactive waste, through-diffusion is probably the most widely used method to determine diffusion parameters of radionuclides in porous media (Maes et al., 2021). In this concept, a clay core is confined in a diffusion cell between two porous filter plates connected to water compartments. One compartment contains the diffusing species (high concentration reservoir, upstream), while the other compartment is free of diffusing species (low concentration reservoir, downstream). The flux arriving at the downstream compartment is monitored. From the evolution of the flux with time, the effective diffusion coefficient D_e and the rock capacity factor $\alpha = \eta R$ with η the accessible porosity and R the retardation factor, can be determined. Besides, the decrease of the concentration of the diffusing species in the upstream compartment can be monitored, as well as the concentration profile inside the clay (by post mortem profiling).

According to Fick's second law, diffusion is characterised by the apparent diffusion coefficient (D_a). D_a is related to the effective diffusion coefficient (D_e) through the capacity factor ηR (eq. (1)):

$$D_e = \eta R D_a \quad (\text{eq. 1})$$

During diffusion experiments, only the product ηR can be determined, not the individual constituents η (accessible porosity) and R (retardation factor). For small neutral tracers, like HTO, as well as for anions, the retardation factor R is taken equal to one (no retardation) reducing the capacity factor equal to the accessible porosity ($\eta R = \eta$). The HTO accessible porosity is the total porosity: $\eta_{HTO} = \eta_{tot}$. For anions, the accessible porosity is lower than the total porosity due to anion exclusion (anions are repelled from the negative charged clay surface; Shackelford and Moore, 2013; Zwahlen et al., 2023) and depends on the ionic strength. For cations, the capacity factor may also be described using a sorption distribution factor (R_d). In such a case, the relationship between ηR and R_d is given via

$$\eta R = \eta + R_d \cdot \rho_b \quad (\text{eq. 2})$$

with ρ_b bulk density and the accessible porosity η is assumed equal to the HTO accessible porosity η_{tot} .

Depending on the experimental conditions concerning the concentration in the up- and downstream reservoirs (Variable Concentration, VC, or Constant Concentration, CC), different sub-types can be defined: CC-CC, VC-VC, VC-CC, CC-VC (Glaus et al., 2015; Aertsens et al., 2017; Takeda et al., 2008a, 2008b). In case of a variable concentration (VC), in the corresponding reservoir the concentration changes according to the flux into (upstream) or out of (downstream) the clay. Even when approximating the concentration in the upstream or downstream reservoir as constant (CC), it remains possible to estimate a concentration change there (see 'parameter estimation' section further on).

A correct mathematical description of these experimental conditions is necessary to provide migration parameters with an acceptably low uncertainty. In addition, a correct implementation of the confining filter plates in the mathematical model is also required. Since the filter plates represent an additional diffusion barrier (in general 1–2 mm at each side of the sample), they should be explicitly accounted for in the modelling,

especially when considering diffusion of strongly sorbing cations, where $D_{e,fil} \ll D_e$ (Glaus et al., 2015; Aertsens et al., 2017). For non-sorbing tracers (anions, HTO) with $D_{e,fil} \geq D_e$, this is less important as long as the clay rock samples are sufficiently thick compared to the combined filter thickness. Many through-diffusion studies (especially older studies) may provide migration parameters, which are subject to a large uncertainty due to the lack of a correct mathematical description of the experimental conditions, incorporating all the possible influences of the filters, strict control of boundary conditions and induced changes at the clay rock interface (Maes et al., 2021). Besides, it is also important to optimise the other experimental properties, like upstream solution volume, sampling frequency downstream, dimensions (diameter, thickness) of the clay rock sample, etc.

Despite the existence of many radionuclide migration studies, it is, however, difficult to compare data when the experiments are not performed on equivalent material due to textural or compositional heterogeneity in natural clay rocks. As a consequence, there are limited or even non-existing studies of diffusion and its parameters on similar samples across different laboratories. Therefore, this study aimed to assess;

- the overall diffusion coefficient data measured on twin samples in two different laboratories,
- the effect of the uncertainties related to the experimental method (through-diffusion) and,
- the effect of modelling approaches on parameter uncertainty

by comparing results from two independent laboratories (R&D group 'Disposal' at SCK CEN and the PSI-LES group) performing through-diffusion experiments with a similar experimental design. This study was part of a benchmark exercise (Van Laer et al., 2022 - NAB 22–23) to support the diffusion programme for Nagra's deep drilling campaign in Switzerland (Van Loon et al., 2023). There, 30 through-diffusion experiments were performed on core samples from Trüllikon1-1 borehole alone along a section of 400 m (depth: 620–1026 m) in order to assess the range in diffusion parameters along the different rock compositions in the framework of Nagra's site selection process. The objective of this study (part 3) was to validate the acceptability of experimental measurement errors in studies of this type. Such cross-lab comparisons are part of confidence building in methodologies, and hence fundamental in the evaluation of transport parameters for host rocks of deep geological nuclear waste repositories.

The significance of this diffusion cross-lab study is multi-fold. Such types of study are useful for verifying the accuracy and reliability of different methods and for identifying potential sources of error or uncertainty. Additionally, the cross-lab comparison of results obtained from similar but not identical methods, allows for conclusions to be drawn regarding the reliability and sensitivity of these approaches. Depending on the specifics of this study, a "baseline" or reference point for future research can be established and the conclusions of this work are contributing to the broader scientific community working with assessments of long-term safe storage of spent fuel and nuclear waste.

Both laboratories have high expertise and experience in performing different types of migration experiments with radionuclides in porous clay media; especially the through-diffusion type for assessing the diffusion behaviour of non-retarded or slightly retarded tracers (Aertsens et al., 2011; 2017; Glaus et al., 2015; Van Loon et al., 2018). For this purpose, through-diffusion experiments of HTO (neutral), $^{36}\text{Cl}^-$ (anionic) and $^{22}\text{Na}^+$ (cationic) were performed by both labs on adjacent subsamples of five clay rock core samples from Trüllikon1-1 (see Mazurek et al., 2023 for sample location). A comprehensive overview of the results obtained in the diffusion studies on >130 dedicated rock samples from 7 sites of Nagra's drilling campaign using these three radionuclides is provided in Van Loon et al. (2023). A specific discussion of the surface diffusion effects for $^{22}\text{Na}^+$ and anion exclusion effects of $^{36}\text{Cl}^-$ in these studies is given in Glaus et al. (2023).

2. Materials and methods

The clay rock samples originate from drill cores from the Trüllikon1-1 borehole in northern Switzerland (see Mazurek et al., 2023 for geological context) at five different depths. For each depth two samples next to each other were subsampled (Table 1). The four samples taken at a depth between 870 and 903 m originate from the Jurassic Opalinus Clay Formation, while the sample at 938 m is from the Staffelegg Formation. The preserved samples were prepared at the University of Bern. A subsample with a diameter of 64 mm was dry drilled perpendicular to the bedding plane from a larger core (95 mm). The sub-core was embedded in epoxy resin (Epofix, Struers, Germany). After hardening at 40 °C overnight, two slices with a thickness of ca. 12–14 mm were prepared by dry cutting, after selecting the slices based on XCT scans (Supporting Information). The samples were selected in a way that they were as homogeneous as possible to meet the criteria of comparability between the two slices. Features such as large pyrite concretions, siderite lenses, macropores, stylolites or burrows, which could affect the experiments, were avoided. All preparations were performed under ambient lab conditions. The samples were put in vacuum bags and distributed to PSI-LES and SCK CEN.

The general approach of the two laboratories was similar (through-diffusion VC-CC type using a similar experimental design), with minor differences in the experimental and modelling approach, and the lab conditions, which all may impact the results. Details of the experimental set-ups are described in Van Laer et al. (2022). After unpacking and visual inspection for possible damage, the samples were weighed, and the diameter and thickness of the clay rock plugs measured. Since the thickness of the clay rock plugs could vary marginally over the plug, it was measured at four positions. The average thickness was used for the modelling. After mounting the clay rock plugs in the diffusion cells, the experimental set-ups were transferred into the glovebox with 400 ppm CO₂ (atmospheric conditions) (more details in Van Loon et al., 2023). At PSI-LES, the glovebox was filled with a mixture of N₂ and CO₂ (400 ± 10 ppm) and the temperature in the glovebox was on average 26.7 ± 0.8 °C. At SCK CEN, the glovebox was filled with Ar and tuned to 400 ppm CO₂ by using an inert working gas Ar containing 400 ppm CO₂ in refreshing/flushing modus. Temperature in the glovebox varied between 21 °C and 24 °C. The concentration of O₂ in the gloveboxes was <0.1 ppm.

Synthetic pore water (SPW) (Table 2) was prepared under anaerobic conditions with degassed water inside the glovebox. The recipe was prepared on the basis of the pore water retrieved via advective displacement (Aschwanden et al., 2021; Kiczka et al., 2023) and is hence close to the in-situ pore water composition (see also Van Loon et al., 2023). All chemicals used were of analytical grade or pure. The target pH value was between 7.6 and 7.8 and was adapted by adding HCl aliquots (~5–50 µL HCl 1 M per liter SPW) in case that pH was increasing in the glovebox before using it for the replacement of the downstream reservoir. During the experiment there was no monitoring of the pH as to minimise disturbance of the experiments.

The diffusion cells used at both institutes had a similar cell design. It consists of two end-cap flanges in which the cylindrical embedded sample is confined (bedding plane perpendicular to direction of diffusion). The flanges have a chamber to place a porous filter disc (stainless steel) which allows the circulation of SPW. AT PSI-LES the cells were made of Ertalyte®, while SCK CEN used stainless steel (316L) cells. The used porous filter discs (stainless steel) had a thickness of L = 1.2 mm at PSI-LES (Bekolut, stainless steel filter 316 L, nominal pore filter size 10 µm) and L = 2 mm at SCK CEN (GKN Filter Technology, SIKAR 5 AX, average pore diameter 11 µm). The porosity of the two filters was similar (~40%). These porous filter plates are in contact with channels in the flanges through which solution from the upstream and downstream reservoir is continuously pumped using a peristaltic pump (IPC, Ismatec, IDEX corporation, USA). Before starting the diffusion experiments, the clay rock samples were re-saturated by circulating SPW at both sides, which was refreshed 4–5 times in a period of 5–6 weeks until the pore

Table 1
Sample characteristics of the five samples from the Trüllikon1-1 borehole used in this study. (WL = water loss porosity at 105 °C measured after the diffusion experiments).

| Sample | Mean depth [m] | System/period | Group | Formation | C (org) [wt.%] | Quartz [wt.%] | K-feldspar [wt.%] | Plagioclase [wt.%] | Calcite [wt.%] | Siderite [wt.%] | Pyrite [wt.%] | Clay minerals [wt.%] | Lithology | Grain density [g/cm ³] | Porosity (WL) PSI | Porosity (WL) SCK CEN ^a |
|--------|----------------|-----------------|--------|----------------|----------------|---------------|-------------------|--------------------|----------------|-----------------|---------------|----------------------|----------------------------|------------------------------------|-------------------|------------------------------------|
| 870 | 870.23 | Middle Jurassic | Dogger | Opalinus Clay | 1.0 | 27 | 6 | 3 | 9 | 3 | 0.7 | 50 | Very sandy/silty claystone | 2.69 | 0.113 | 0.055 |
| 882 | 882.36 | | | | 1.1 | 22 | 5 | 3 | 7 | 5 | 0.1 | 57 | | 2.70 | 0.133 | 0.116 |
| 890 | 890.39 | | | | 1.1 | 23 | 6 | 2 | 7 | 3 | 0.1 | 57 | | 2.68 | 0.123 | 0.055 |
| 902 | 902.85 | | | | 1.1 | 24 | 5 | 3 | 7 | 5 | 0.1 | 55 | | 2.69 | 0.127 | 0.095 |
| 938 | 938.90 | Early Jurassic | Lias | Staffelegg Fm. | 4.7 | 10 | 3 | 2 | 43 | 0 | 1.8 | 36 | Calcareous marl | 2.53 | 0.097 | 0.089 |

^a Values of samples 870 and 890 are assumed to be too low (no explanation found).

Table 2
Composition of the synthetic pore water (SPW).

| Element | Concentration (M) |
|--------------------------|-----------------------|
| Na | 2.44×10^{-1} |
| K | 1.64×10^{-3} |
| Ca | 2.22×10^{-2} |
| Mg | 1.56×10^{-2} |
| Sr | 2.89×10^{-4} |
| Cl | 2.72×10^{-1} |
| S (as SO ₄) | 2.43×10^{-2} |
| C (as HCO ₃) | 4.87×10^{-4} |
| pH | 7.68 |
| Ionic strength (M) | 0.354 |

water chemistry was stable (follow-up pore water chemistry in Van Laer et al., 2022).

For the diffusion measurements (VC-CC type) the upstream reservoir (100 mL glass flask) was filled with 100 mL SPW spiked with radionuclides. The downstream reservoir (20 mL polyethylene vial) was filled with 10 (PSI-LES) or 15 mL (SCK CEN) SPW. The solution at the downstream side was replaced regularly at a time interval Δt of approximately 2–3 days to keep the concentration of the tracer in this compartment as low as possible. In a first series, diffusion experiments were performed with HTO and $^{36}\text{Cl}^-$ (activity ca. 500 Bq/mL). In a second stage, diffusion of $^{22}\text{Na}^+$ was measured (activity ca. 500 (SCK CEN) or 200 (PSI-LES) Bq/mL). HTO and $^{36}\text{Cl}^-$ were analysed with Liquid Scintillation Counting, while $^{22}\text{Na}^+$ was measured with gamma counting. At the end of the experiments, the water content was determined by weighing the clay rock samples before and after drying at 105 °C until constant weight. After accounting for the water loss of the resin, the water loss porosity could be calculated. The determination of the uncertainties is explained in detail in Van Laer et al. (2022) and Van Loon and Soler (2003).

2.1. Parameter estimation

The diffusion parameters are estimated by solving numerically (with Comsol Multiphysics® software) the diffusion-advection equation, involving a 1D-linear geometry for the filter and the clay rock domains. Best-fit parameter values are obtained from a parameter optimisation routine. The concentration changes in the upstream solution reservoir are reflected in variable (concentration, VC) boundary conditions at the interface between filter and solution while a constant (zero) concentration (CC) boundary condition was assumed for the downstream side. The tracer concentration in the upstream reservoir decreases according to the diffusive flux into the porous medium (Glaus et al., 2015; Van Laer et al., 2022). Although for the downstream boundary condition a constant zero tracer concentration is assumed, a non-zero downstream concentration C_{down} can be calculated by integrating the downstream flux over the duration of a downstream measurement. If this duration is sufficiently small, the downstream concentration C_{down} remains much smaller than the upstream concentration, justifying for the downstream boundary condition the approximation of a zero concentration.

The modelling approaches of SCK CEN and PSI-LES are very similar, but have three main differences. The first difference is the choice of the fit parameters. SCK CEN optimised the D_a and ηR values and derived subsequently D_e by $D_e = \eta R D_a$. PSI-LES fitted D_e instead of D_a and used for ηR a tracer dependent approach. In case of HTO and $^{36}\text{Cl}^-$, the accessible porosity η ($=\eta R$ because $R = 1$) is optimised, but for the sorbing $^{22}\text{Na}^+$ tracer the R_d (sorption distribution coefficient) is fitted, which can be converted to ηR according to equation (2) with η and ρ_b determined from the HTO diffusion data ($\eta = \eta_{\text{tot}}$).

Second, different experimental data are fitted. PSI-LES optimised simultaneously the upstream concentration (Bq/mL) and the total diffused mass at the downstream side (Bq) (cumulative activity of all previous sample activities corrected for radioactive decay). SCK CEN

fitted the up- and downstream concentration (Bq/mL) simultaneously. Note that the concentration in the downstream reservoir depends on the duration of the sampling period between two replacements. After each measurement and the corresponding replacement of the downstream reservoir, the concentration in the downstream reservoir is put to zero, after which it increases again. This can result in an irregular course of the concentration with time due to varying sampling times. Instead of plotting the ‘shark tooth’ model (Aertsens et al., 2017; Glaus et al., 2015) only the fitted points at each measurement (replacement) are plotted and connected with each other (Fig. 1). To provide a more comprehensive understanding, the flux in the downstream reservoir is also presented, as it eliminates the time-dependency. Because the cumulative activity is derived from the downstream concentration, both quantities contain the same basic information. Fitting one or the other, leads to negligible numerical differences between the corresponding sets of optimal values.

Third, SCK CEN and PSI-LES take different values for the diffusion parameters of the filters. PSI-LES assumes the capacity factor of the filter is equal to the filter porosity: $\eta R_{\text{fil}} = 0.4$. For the implementation of the filters in the model, PSI-LES used for HTO experience values from other filters (Glaus et al., 2008): $5 \times 10^{-11} \text{ m}^2 \text{ s}^{-1} < D_{e,\text{fil}} < 1.5 \times 10^{-10} \text{ m}^2 \text{ s}^{-1}$ (preferred value: $1.0 \times 10^{-10} \text{ m}^2 \text{ s}^{-1}$). For $^{22}\text{Na}^+$, the applied effective diffusion coefficient for the filters is $6 \times 10^{-11} \text{ m}^2 \text{ s}^{-1}$, with $3 \times 10^{-11} \text{ m}^2 \text{ s}^{-1}$ and $9 \times 10^{-11} \text{ m}^2 \text{ s}^{-1}$ as the lower and upper bounding values, derived from the proportionality of the aqueous bulk diffusion coefficients of the respective tracers and furthermore consistent with experience values (Aldaba et al., 2014). The uncertainty ranges for the experience values were chosen rather large in order to cover the potential variability among different production batches (Glaus et al., 2008). These upper and lower limits were used for two ‘bounding’ parameter optimisation scenarios. The optimal values for clay rock diffusion parameters were calculated as the average of the two bounding ‘filter scenarios’. In the case of $^{36}\text{Cl}^-$, a $D_{e,\text{fil}}$ value of $1.0 \times 10^{-10} \text{ m}^2 \text{ s}^{-1}$ was used, but no sensitivity analysis was carried out for the filter diffusivities in view of the very low effective diffusivities of this tracer in the clay rock.

At SCK CEN two options were used for the filter diffusion parameters: (i) fixed filter parameters (FF), which like the PSI-LES approach takes constant (fixed) filter parameter values, and (ii) assuming the same diffusion parameters for filter and clay (F=C) (in order to reduce the amount of parameters). For the FF option, the previously determined values of $\eta R_{\text{fil}} = 0.4$ and $D_{a,\text{fil}} = 3.5 \times 10^{-10} \text{ m}^2/\text{s}$ (Aertsens et al., 2011) were taken, corresponding to $D_{e,\text{fil}} = 1.4 \times 10^{-10} \text{ m}^2/\text{s}$, which is very close to the upper limit for $D_{e,\text{fil}}$ of PSI-LES ($1.5 \times 10^{-10} \text{ m}^2/\text{s}$). For $^{36}\text{Cl}^-$ and $^{22}\text{Na}^+$, the values of the filter diffusion parameters were not determined experimentally before and the values for HTO were used for simplicity.

The second SCK CEN approach is to assume that the diffusion parameters in filter and clay are equal (F=C). This approach was previously justified for Boom Clay samples perpendicular to the bedding (Aertsens et al., 2011), where clay rock and filter parameters were indeed nearly the same. The fit results will make clear if this assumption is also valid or not for the Jurassic samples of Switzerland in this study.

In order to verify both models and to assess the uncertainties on the modelling, both institutes fitted each other’s datasets for HTO and $^{36}\text{Cl}^-$. SCK CEN optimised the PSI-LES dataset with the FF approach using the preferred value $D_{e,\text{fil}} = 1.0 \times 10^{-10} \text{ m}^2 \text{ s}^{-1}$ and $\eta R_{\text{fil}} = 0.4$. PSI-LES fitted the SCK CEN data with the minimum and maximum bounding values of 0.7 and $2.1 \times 10^{-10} \text{ m}^2/\text{s}$ for the $D_{e,\text{fil}}$ value used by SCK CEN: $D_{e,\text{fil}} = 1.4 \times 10^{-10} \text{ m}^2/\text{s}$.

3. Results

Figs. 1 and 2 depict the graphic presentation of the data using only one representative sample (882), while the specifics of the remaining samples can be found in Van Laer et al. (2022). For the SCK CEN sample

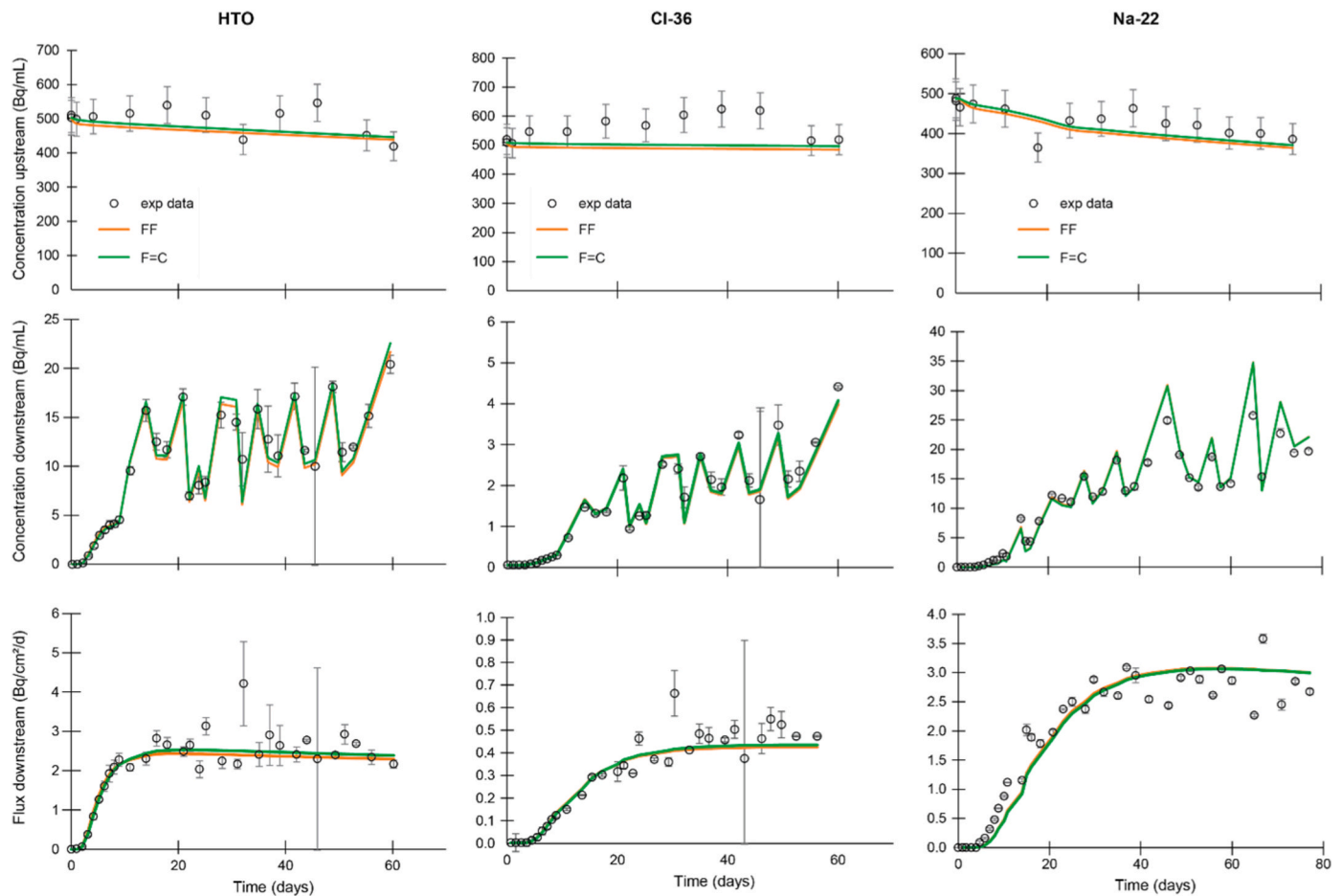


Fig. 1. Experimental data (symbols) and fits (FF orange line, F=C green line) of sample 882 obtained by SCK CEN for HTO, $^{36}\text{Cl}^-$ and $^{22}\text{Na}^+$ diffusion show (i) the evolution of the inlet concentration (Bq/mL), (ii) the evolution of the downstream concentration (Bq/mL) (the lines of the fits present only the fit values at measurement time and not the complete 'shark tooth' model with zero concentrations between the two consecutive points) and (iii) the evolution of the downstream flux (Bq/cm²/d).

870, the corresponding experimental data were not fitted as preferential flow was observed (possibly caused during sample preparation by screwing the plugs tighter to prevent leakage). Similarly, SCK CEN sample 890 showed irregular data after 21 days due to experimental artefacts, so it was deemed necessary to use a reduced dataset comprising data only up to day 21. Therefore, when interpreting the results, it is important to keep this in mind. Further, the very dry conditions in the glovebox at SCK CEN caused a slight evaporation of the solution at the upstream side during the experiment (up to 15% by the end of the experiment), resulting in a slight up-concentration for ^{36}Cl and ^{22}Na at the end (Fig. 1). The limited decrease in activity for ^{36}Cl resulted in a slight increase in concentration. In the case of ^{22}Na the impact of the evaporation is not discernible, as the activity decrease due to diffusion is larger. For HTO there is no up-concentration increase because it evaporates proportionally. Nevertheless, these concentration changes have a negligible influence on the modelling outcome as the primary determinant is the fitting of the downstream reservoir.

Table 3 summarises the obtained diffusion parameters, which are presented also graphically in Fig. 3. For the PSI data of HTO and $^{22}\text{Na}^+$, a single best-fit value obtained as the average of the two bounding scenarios of filter diffusion properties is provided. The specified uncertainties comprise the propagation of the basic fit errors and the variability of D_e values for the two bounding cases. For the $^{36}\text{Cl}^-$ data, only the fit errors are given in view of the negligible contribution of the filters to overall diffusion. For the SCK CEN data, two results for the different scenarios regarding the diffusive properties of the confining filter (F=C, FF) are given. Clearly, diffusion in the filters ($D_{e,fil} = 1.4 \times$

$10^{-10} \text{ m}^2/\text{s}$) was much faster than in the rock samples (for HTO $D_e \approx 3\text{--}10 \times 10^{-12} \text{ m}^2/\text{s}$), making the F=C approach not an ideal approximation here. The two bounding assumptions for the filter properties can be regarded as symmetrically distributed around the best-guess assumption in the case of the PSI data. For this reason, the results obtained thereby were averaged. This procedure was not applicable in the case of the SCK CEN data. The FF approach is regarded as the best-estimate scenario for the filters, while the F=C case was carried out for a comparison of former assumptions applicable for Boom Clay. For this reason, the results of the FF approach are considered as the best-estimate for the clay rock diffusion properties and accordingly, only the results of the FF scenario will be used in the following for comparison with the PSI average data.

The uncertainties associated with the PSI-LES parameters of HTO and $^{22}\text{Na}^+$ are determined by the chosen filter uncertainties, while for their $^{36}\text{Cl}^-$ parameters and the parameters of SCK CEN the uncertainty presented is the fit error, which indicates the accuracy of the data fitting, and generally underestimates the uncertainty associated with the diffusion parameter itself.

The D_e values for HTO for samples 890, 902 and 938 (Table 3) show excellent agreement between PSI-LES and SCK CEN. However, sample 882 of SCK CEN shows slightly lower values compared to PSI-LES. When comparing the η values, the porosities obtained by SCK CEN are slightly lower than the porosities obtained for PSI-LES and correspond very well with the porosities determined by water loss (WLP) (Table 1), where also slightly lower values were observed for the SCK CEN samples (disregarding WLP of 870 and 890).

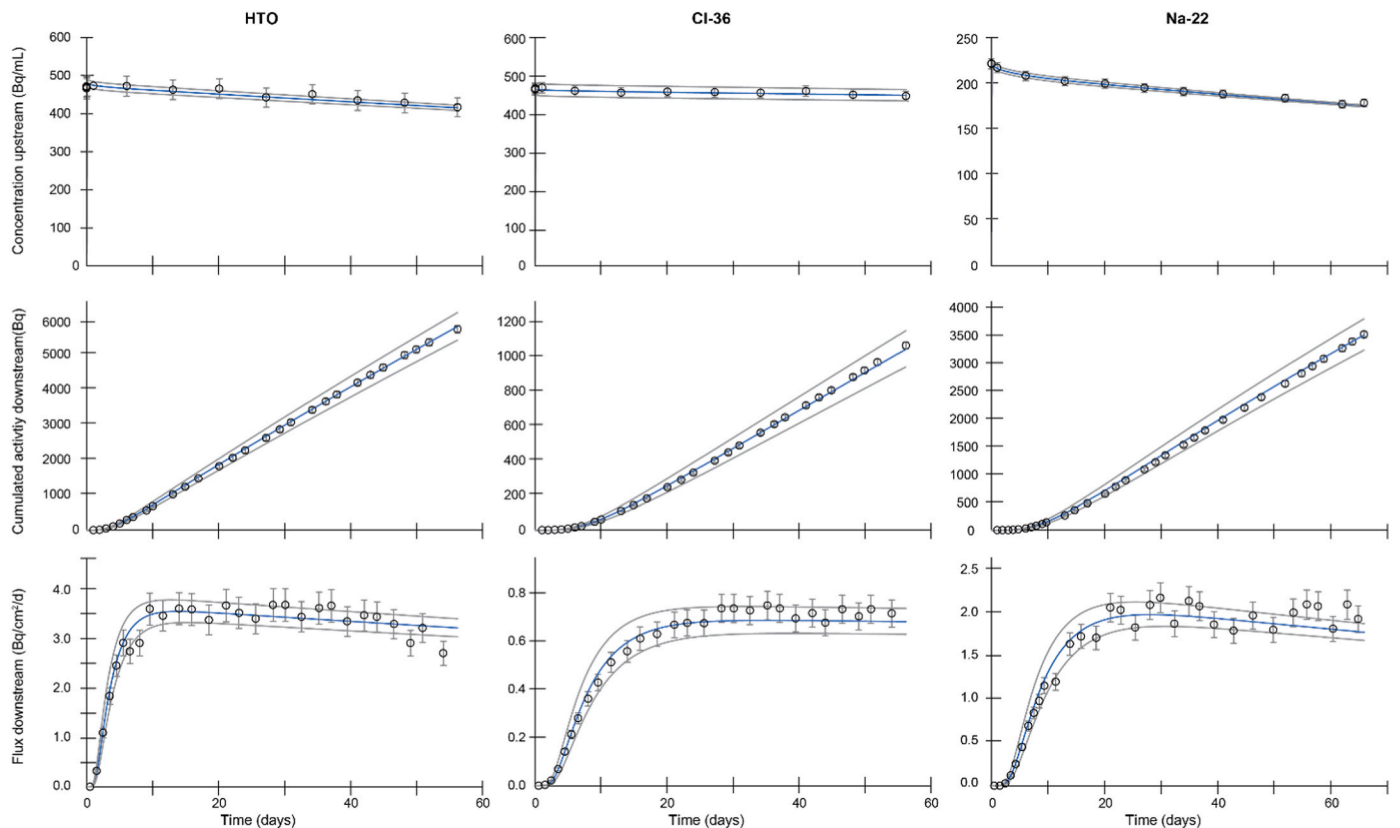


Fig. 2. Experimental data (points) and fits (line) of sample 882 obtained by PSI-LES for HTO, $^{36}\text{Cl}^-$ and $^{22}\text{Na}^+$ diffusion show (i) the evolution of the inlet concentration (Bq/mL), (ii) the accumulated mass downstream (Bq) and (iii) the evolution of the downstream flux (Bq/cm²/d).

For $^{36}\text{Cl}^-$, the D_e values of samples 902 and 938 are very comparable between the two laboratories, while the value of sample 882 differs slightly, but still less than a factor 2 (Table 3). For the reduced dataset of sample 890, the obtained parameters by SCK CEN for D_e are a factor 2 to 2.5 higher. The higher flux at the downstream side (± 2.5 –3 times compared to sample 882 and 890) explains this higher D_e value, while this is not expected based on the HTO data where similar fluxes were observed for the samples 882, 890 and 902 (details in Van Laer et al., 2022). No explanation was found for this observation. The porosities of these samples agree very well with each other, except for sample 902 where the porosities determined by SCK are 2–3 times lower than the values obtained by PSI-LES. The most plausible explanation is that these experimental data are not compatible with the model over the complete time interval, which could lead to an underestimation of the parameter. The lower porosities determined for $^{36}\text{Cl}^-$ compared to HTO (between 26% and 51% of the HTO porosity) confirm the anion exclusion effect (Table 3).

For $^{22}\text{Na}^+$, the D_e values obtained by both institutes are closely comparable. Also, the capacity factors ηR (converted from the fitted R_d in case of PSI-LES) correspond very well for the samples 890, 902 and 938. In case of sample 882 the capacity factors determined by SCK CEN are slightly higher than the values obtained by PSI-LES, but the difference is still lower than a factor 2.

In general, sample 938 (Staffelegg Formation) has slightly lower effective and apparent diffusion coefficients than the four other cores from the Opalinus Clay (Table 3). This is in line with the lower clay content of this sample (Table 1) and the lower water porosity, between which a clear positive correlation is shown in Van Loon et al. (2023).

To assess the variations between the modelling approaches on the same dataset, the diffusion datasets of HTO and $^{36}\text{Cl}^-$ from SCK CEN and PSI-LES were exchanged for modelling. Table 4 presents a comparison of the results. The optimal values obtained for the PSI-LES data differ a

maximum of 5% for samples 870, 882, 890 and 902 between the fits of both institutes. Only for sample 938, the difference is higher (e.g. 12% for D_e and 25% for ηR). For the SCK CEN data the differences between the fit results from SCK CEN and PSI-LES are slightly higher, although still small, ranging between 3 and 23% for D_e and between 3 and 45% for ηR , with the highest difference again for sample 938. Fig. 4 illustrates for sample 882 the good correspondence between the D_e values of the two modelling approaches. The observed differences are significantly smaller than the differences between the two experiments (see Table 4).

4. Discussion

In order to compare the diffusion parameters, the deviations between the best-estimates of both institutes were determined (Table 5). The average deviation for the different radionuclides and experiments is 30% for the D_e (ranging between 0 and 73%) and 28% for ηR (ranging between 2 and 125%).

Different reasons can be given to explain the slight deviations between the results of the two institutes. First, there was an evaluation made on the temperature effect, since there was a slight difference in the ambient temperature at which the experiments were performed. The experiments at PSI-LES were performed at a slightly higher temperature (26.7 ± 0.8 °C) than at SCK CEN (T varied between 21 and 24 °C). Diffusion is a temperature dependent process and the temperature dependency can be described by the Arrhenius Law: $D_e = A \cdot e^{-E_a/RT}$ with A the pre-exponential factor, $R = 8.314$ J/(K mol) the molar gas constant and E_a the activation energy (kJ/mol). According to this law and assuming an activation energy of 20 kJ/mol (Van Loon et al., 2005), the diffusion coefficient D_e of HTO at (PSI-LES) is about 8 (for 24 °C) to 17 (for 21 °C) percent higher than the diffusion coefficient determined at SCK CEN. When performing a temperature correction of 10%, the difference between the results of the institutes becomes significantly lower

Table 3

Overview of fitted and derived diffusion parameters (D_a , ηR , D_e). SCK CEN gives the parameter values for two modelling approaches (F=C and FF) with the fit errors as uncertainty range. For the PSI-LES datasets, the best-estimate value is given. For HTO and $^{22}\text{Na}^+$ the uncertainty range are the parameters obtained with the minimum and maximum $D_{e,fit}$. For $^{36}\text{Cl}^-$ the uncertainties are representing the fit errors. Derived parameters (D_e in case of SCK CEN and D_a and ηR_{Na} in case of PSI-LES) are given in italics. The errors on the calculated parameters are determined via error propagation.

| Sample | Exp data | HTO | | | $^{36}\text{Cl}^-$ | | | $^{22}\text{Na}^+$ | | |
|--------|-----------------------|--|---------------|--|--|---------------|--|--|----------------|--|
| | | D_a ($\times 10^{-11}$ m ² /s) | η (-) | D_e ($\times 10^{-12}$ m ² /s) | D_a ($\times 10^{-11}$ m ² /s) | η (-) | D_e ($\times 10^{-12}$ m ² /s) | D_a ($\times 10^{-11}$ m ² /s) | ηR^a (-) | D_e ($\times 10^{-12}$ m ² /s) |
| 870 | PSI | 6.3 ± 0.4 | 0.121 ± 0.007 | 7.6 ± 0.2 | 2.9 ± 0.2 | 0.053 ± 0.003 | 1.5 ± 0.07 | 2.3 ± 0.2 | 0.41 ± 0.02 | 9.5 ± 0.4 |
| | FF | | | | | | | | | |
| | F=C | | | | | | | | | |
| 882 | PSI | 9.2 ± 0.7 | 0.134 ± 0.009 | 12.3 ± 0.5 | 4.0 ± 0.3 | 0.060 ± 0.004 | 2.4 ± 0.1 | 3.7 ± 0.3 | 0.44 ± 0.03 | 16.6 ± 0.9 |
| | SCK (FF) | 7.6 ± 0.08 | 0.111 ± 0.005 | 8.46 ± 0.4 | 2.7 ± 0.03 | 0.050 ± 0.002 | 1.4 ± 0.06 | 1.8 ± 0.03 | 0.720 ± 0.049 | 13.0 ± 0.9 |
| | SCK (FC) | 10.8 ± 0.4 | 0.101 ± 0.006 | 10.9 ± 0.8 | 4.3 ± 0.09 | 0.041 ± 0.002 | 1.8 ± 0.09 | 2.8 ± 0.06 | 0.576 ± 0.046 | 16.0 ± 1.3 |
| 890 | PSI | 7.3 ± 0.5 | 0.129 ± 0.008 | 9.4 ± 0.3 | 3.4 ± 0.2 | 0.058 ± 0.003 | 2.0 ± 0.07 | 2.7 ± 0.2 | 0.42 ± 0.02 | 11.6 ± 0.5 |
| | SCK ^b (FF) | 7.1 ± 0.3 | 0.117 ± 0.015 | 8.3 ± 1.1 | 6.7 ± 0.8 | 0.059 ± 0.014 | 4.0 ± 1.0 | 2.5 ± 0.06 | 0.436 ± 0.043 | 10.8 ± 1.1 |
| | SCK ^b (FC) | 10.4 ± 0.6 | 0.110 ± 0.016 | 11.4 ± 1.8 | 10.8 ± 1.4 | 0.047 ± 0.003 | 5.0 ± 1.4 | 4.0 ± 0.2 | 0.346 ± 0.040 | 13.7 ± 1.7 |
| 902 | PSI | 6.0 ± 0.4 | 0.134 ± 0.007 | 8.1 ± 0.3 | 2.6 ± 0.1 | 0.058 ± 0.002 | 1.5 ± 0.04 | 2.3 ± 0.1 | 0.46 ± 0.02 | 10.5 ± 0.4 |
| | SCK (FF) | 6.7 ± 0.2 | 0.099 ± 0.006 | 6.6 ± 0.4 | 5.3 ± 0.4 | 0.026 ± 0.001 | 1.4 ± 0.1 | 1.8 ± 0.02 | 0.383 ± 0.013 | 6.9 ± 0.2 |
| | SCK (FC) | 10.3 ± 0.4 | 0.083 ± 0.005 | 8.5 ± 0.6 | 8.9 ± 0.7 | 0.020 ± 0.003 | 1.8 ± 0.3 | 3.0 ± 0.05 | 0.306 ± 0.012 | 9.0 ± 0.4 |
| 938 | PSI | 3.2 ± 0.4 | 0.092 ± 0.009 | 3.0 ± 0.2 | 1.4 ± 0.4 | 0.035 ± 0.008 | 0.49 ± 0.07 | 0.94 ± 0.05 | 0.28 ± 0.01 | 2.6 ± 0.07 |
| | SCK (FF) | 3.0 ± 0.08 | 0.084 ± 0.007 | 2.5 ± 0.2 | 1.5 ± 0.02 | 0.033 ± 0.003 | 0.49 ± 0.04 | 1.1 ± 0.02 | 0.185 ± 0.010 | 2.0 ± 0.1 |
| | SCK (FC) | 4.7 ± 0.2 | 0.070 ± 0.007 | 3.3 ± 0.4 | 2.4 ± 0.08 | 0.029 ± 0.003 | 0.68 ± 0.07 | 1.4 ± 0.03 | 0.174 ± 0.010 | 2.4 ± 0.2 |

^a PSI fits R_d instead of ηR values: conversion is made via equation $\eta R = \eta + R_d \rho_b$ with η and ρ_b obtained from HTO diffusion.

^b 21 days for HTO and ^{36}Cl .

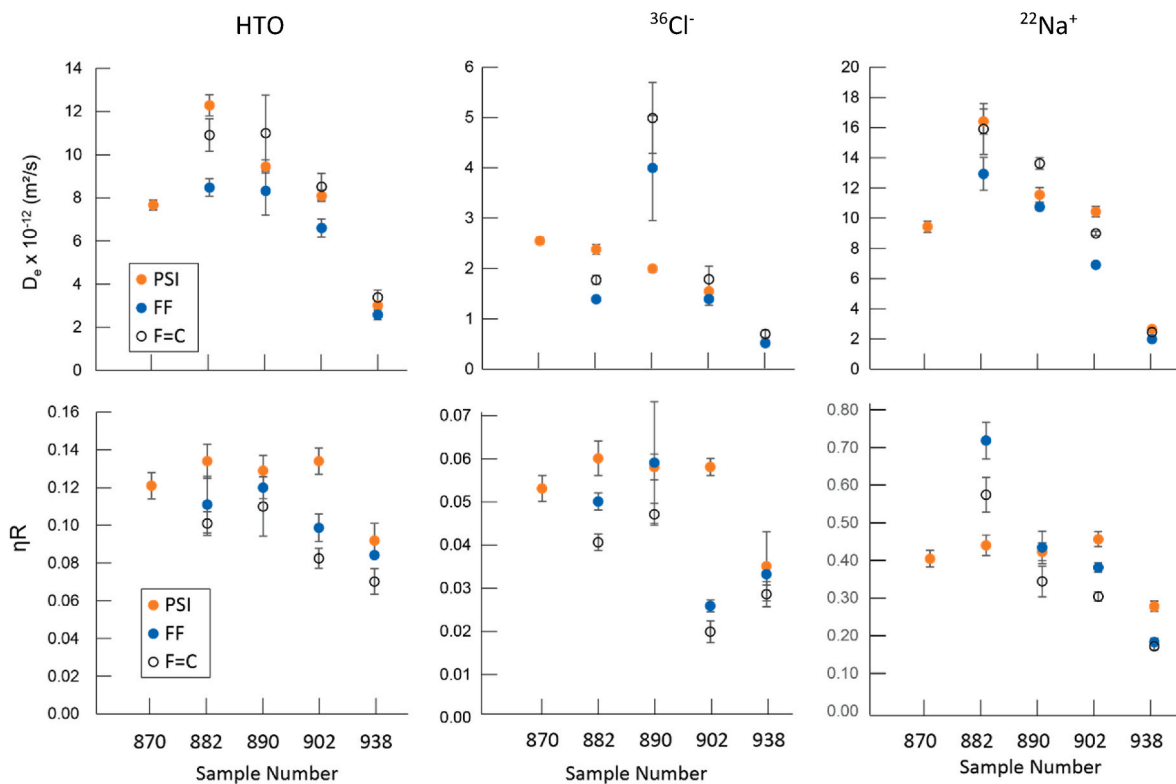


Fig. 3. Diffusion parameters of HTO, $^{36}\text{Cl}^-$ and $^{22}\text{Na}^+$ obtained for the twin samples (882, 890, 902, 938) by SCK CEN (approaches FF (blue) and F = C (open symbol) with the fit errors as uncertainty range) and by PSI-LES (average values (orange) - the uncertainty range for HTO and $^{22}\text{Na}^+$ represents the parameters obtained with the minimum and maximum $D_{e,fit}$; for $^{36}\text{Cl}^-$ the uncertainties are representing the fit errors). The PSI-LES capacity factors ηR of $^{22}\text{Na}^+$ are converted from the fitted R_d value.

Table 4

Overview of diffusion parameters of the experimental datasets of HTO and $^{36}\text{Cl}^-$ determined by the modelling approaches of both institutes: FF approach for SCK CEN and average value of minimum and maximum bounding values for PSI-LES. Calculated parameters (D_a in case of PSI – D_e in case of SCK CEN) are given in italics.

| Sample | Modelling approach | HTO | | | $^{36}\text{Cl}^-$ | | |
|--------------------------------------|--------------------|--|-----------|--|--|-----------|--|
| | | D_a ($\times 10^{-11}$ m ² /s) | $\eta(-)$ | D_e ($\times 10^{-12}$ m ² /s) | D_a ($\times 10^{-11}$ m ² /s) | $\eta(-)$ | D_e ($\times 10^{-12}$ m ² /s) |
| Parameters of PSI dataset | | | | | | | |
| 870 | PSI - average | 6.3 | 0.121 | 7.64 | 2.9 | 0.053 | 1.54 |
| | SCK - FF | 6.3 | 0.124 | 7.86 | 3.0 | 0.051 | 1.54 |
| 882 | PSI - average | 9.2 | 0.134 | 12.30 | 4.0 | 0.060 | 2.37 |
| | SCK - FF | 9.2 | 0.137 | 12.60 | 4.0 | 0.059 | 2.40 |
| 890 | PSI - average | 7.3 | 0.129 | 9.44 | 3.4 | 0.058 | 1.98 |
| | SCK - FF | 7.3 | 0.133 | 9.71 | 3.5 | 0.057 | 2.00 |
| 902 | PSI - average | 6.0 | 0.134 | 8.07 | 2.6 | 0.058 | 1.53 |
| | SCK - FF | 6.1 | 0.137 | 8.30 | 2.7 | 0.057 | 1.53 |
| 938 | PSI - average | 3.2 | 0.092 | 2.95 | 1.4 | 0.035 | 0.49 |
| | SCK - FF | 3.6 | 0.076 | 2.72 | 1.6 | 0.028 | 0.44 |
| Parameters of SCK CEN dataset | | | | | | | |
| 882 | PSI - average | 7.0 | 0.135 | 9.38 | 2.6 | 0.054 | 1.41 |
| | SCK - FF | 7.6 | 0.111 | 8.46 | 2.7 | 0.050 | 1.37 |
| 890 | PSI - average | 6.2 | 0.158 | 9.76 | 7.1 | 0.061 | 4.31 |
| | SCK - FF | 7.1 | 0.117 | 8.34 | 6.7 | 0.059 | 3.96 |
| 902 | PSI - average | 6.2 | 0.117 | 7.27 | 5.9 | 0.021 | 1.21 |
| | SCK - FF | 6.7 | 0.099 | 6.56 | 5.3 | 0.026 | 1.37 |
| 938 | PSI - average | 2.5 | 0.122 | 3.08 | 1.6 | 0.029 | 0.45 |
| | SCK - FF | 3.0 | 0.084 | 2.51 | 1.5 | 0.033 | 0.49 |

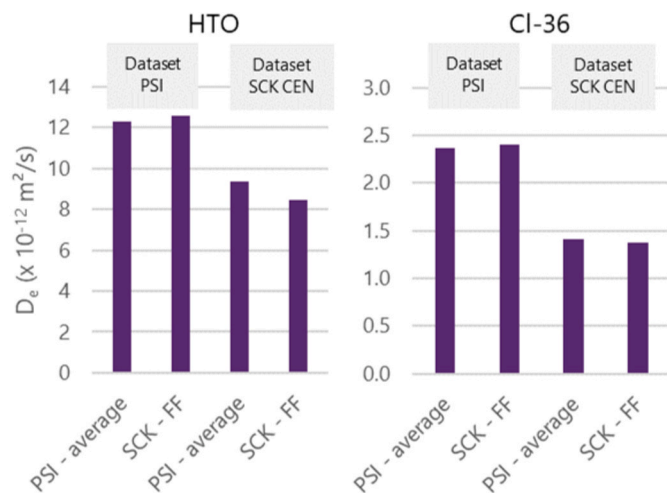


Fig. 4. Effective diffusion coefficient of HTO and $^{36}\text{Cl}^-$ determined for the two datasets of sample 882 and modelled by the two modelling approaches (PSI-LES: average of minimum and maximum bounding values – SCK CEN: FF approach).

with an average of 20% and values varying between 1 and 56% (Table 5). This shows that it is important to take into account the difference in temperature when comparing diffusion coefficients, even if the T difference of the laboratory setting is only a few degrees. Importantly, the difference in thickness of the filters is not considered a reason for the discrepancies, because the impact of the filters is explicitly taken into account during the modelling procedures (see also Glaus et al., 2015).

Next to the differences on experimental level, the study aimed also to evaluate the uncertainty caused by the modelling. As explained in the results section, the different modelling approaches add to the overall discrepancies, but their contribution is very limited and clearly less than the overall observed discrepancies.

The remaining deviation can potentially be attributed to local sample heterogeneity, which is more significant in case of thin samples (like in this study). The XCT scans of the clay rock cores (Supporting Information) showed some heterogeneities between the two slices. Further, the small differences in water porosity (obtained by WLP and diffusion

experiments) might be an indication for heterogeneity as well. Aschwanden et al. (2021) observed also differences larger than uncertainty within the cm scale on different TRU1 samples. Due to heterogeneity, the sample slices – although taken next to each other – might have slightly different structural and diffusive properties. Quantifying the impact of minute heterogeneity within these diffusion samples proves to be a challenging task.

Finally, the deviations or data discrepancies among the institutes were compared to the variability observed in through-diffusion experiments performed on duplicate samples within the same institute (PSI-LES) (Van Loon, 2014; Van Loon et al., 2023). Figure 6 in the Supporting Information shows the D_e values for HTO, $^{36}\text{Cl}^-$ and $^{22}\text{Na}^+$ for five sets of twin samples. Since the experimental conditions and modelling approach were identical for these duplicate samples, any variability observed can only be attributed to sample heterogeneity or the uncertainties associated with the experiment procedure. Similar

Table 5

Deviations (%) between SCK CEN and PSI-LES parameters of effective diffusion coefficients (D_e) and capacity factors (ηR) determined as the absolute difference between the best estimate values of SCK CEN (FF approach) and PSI-LES relative to the value of SCK CEN. For D_e the deviation is determined for the temperature (T) corrected value of PSI-LES (10%) as well. In general SCK CEN values tend to be lower than PSI-LES, but for a few values (underlined) the reverse is true.

| Sample | RN | Deviation (%) | | ηR |
|----------------|-----|---------------|--------------------------|-----------|
| | | D_e | | |
| | | uncorrected | corrected for ΔT | |
| 882 | HTO | 45 | 30 | 21 |
| | Cl | 73 | 56 | 20 |
| | Na | 28 | 15 | <u>39</u> |
| 890 | HTO | 13 | 2 | <u>10</u> |
| | Cl | 50 | 55 | <u>2</u> |
| | Na | <u>7</u> | <u>3</u> | <u>3</u> |
| 902 | HTO | 23 | 11 | 36 |
| | Cl | 12 | 1 | 125 |
| | Na | 52 | 36 | 20 |
| 938 | HTO | 18 | 6 | 9 |
| | Cl | 0 | <u>10</u> | 6 |
| | Na | 35 | 21 | 51 |
| Average | | 30 | 20 | 28 |

deviations ranging from 1 to 93%, but mostly below 30%, were observed, which aligns with the variability observed here among the two institutes.

5. Conclusion

In this cross-lab study, through-diffusion experiments were performed on five twin samples (two sample slabs from the same core) of Jurassic clay-rich samples (Opalinus Clay and Staffelegg Formation) from the Trüllikon 1-1 borehole (Northern Switzerland) in two independent laboratories (SCK CEN and PSI-LES). This was done for three different types of tracers, respectively a neutral (HTO), an anionic ($^{36}\text{Cl}^-$) and a cationic species ($^{22}\text{Na}^+$). The experimental design and methodology at SCK CEN and PSI-LES were (very) comparable, but there were some differences, such as temperature, filter thickness and modelling approaches.

The cross-lab study demonstrated a notable agreement between the results obtained from diffusion measurements from both institutes. In most cases, the difference between the effective diffusion coefficient D_e and capacity factor ηR for each of the three radionuclides was consistently (except for one outlier) less than a factor 2 (<100%), with even lower differences observed (30% for D_e and 28% for ηR). This level of difference is comparable to the intrinsic variability observed between diffusion values obtained from through-diffusion experiments performed by the same institute on twin samples.

The evaluation of the best-fit parameter values and the cross-fitting comparison showed that the discrepancies can partially be attributed to differences in experimental conditions (mainly the difference in temperature that could explain 8–17% of the deviation) and partially by the model approach (chosen filter parameters, fitting optimisation strategy), with the experimental conditions assumed to have the largest effect. Furthermore, it has to be emphasised that the upper ranges of discrepancy are rather above the uncertainty limits of the best-fit parameter values. The most obvious explanation for such findings are probably local heterogeneities among the twin samples. The good agreement of the best-fit parameter values obtained for the majority of the samples and the remarkably consistent results within the expected robustness of the experimental and computational methods, provides confidence in this kind of through-diffusion approach to determine these important transport parameters in argillaceous rocks. The data provide robust evidence that both methods addressed the potential issues that can create large uncertainty, as mentioned in the introduction.

Reliable, auditable and transparent data analysis to assess accurately transport parameters (e.g. diffusive behaviour) is paramount for any safety assessment and the evaluation of the long-term performance of nuclear waste repositories. The outcome of the present study, viz. the relatively small uncertainties within the methodological approaches provides much confidence for applications of the diffusion parameters in radionuclide transport models.

Declaration of competing interest

The authors declare the following financial interests/personal relationships which may be considered as potential competing interests:

Liesbeth Van Laer reports financial support and writing assistance were provided by Nagra.

Data availability

Data will be made available on request.

Acknowledgements

We would like to thank several people for their contribution of this study including lab technicians at SCK-CEN and PSI-LES as well as Carmen Zwahlen of the University of Bern for support with the samples.

Thanks go also to Bernd Grambow for an earlier review. The study was funded through Nagra (Nationale Genossenschaft für die Lagerung radioaktiver Abfälle), Switzerland.

Appendix A. Supplementary data

Supplementary data to this article can be found online at <https://doi.org/10.1016/j.apgeochem.2023.105840>.

References

- Aertsens, M., Govaerts, J., Maes, N., Van Laer, L., 2011. Consistency of the strontium transport parameters in Boom Clay obtained from different types of migration experiments: accounting for the filter plates. *Mater. Res. Soc. Symp. Proc.* 1475, 583–588.
- Aertsens, M., Van Laer, L., Maes, N., Govaerts, J., 2017. An improved model for through-diffusion experiments: application to strontium and tritiated water (HTO) diffusion in Boom Clay and compacted illite. *Geological Society, London, Special Publications* 443, 205–210.
- Aldaba, D., Glaus, M.A., Leupin, O., Van Loon, L.R., Vidal, M., Rigol, A., 2014. Suitability of various materials for porous filters in diffusion experiments. *Radiochim. Acta* 102, 723–730.
- Aschwanden, L., Camesi, L., Gimmi, T., Jenni, A., Kiczka, M., Mäder, U., Mazurek, M., Rufer, D., Waber, H.N., Wersin, P., Zwahlen, C., Traber, D., 2021. TBO Trüllikon-1-1: Data Report Dossier VIII: Rock Properties, Porewater Characterisation and Natural Tracer Profiles. *Arbeitsbericht NAB 20-09*. NAGRA, Wettingen, Switzerland.
- Glaus, M.A., Rossé, R., Van Loon, L., Yaroshchuk, A., 2008. Tracer diffusion in sintered stainless steel filters: measurement of effective diffusion coefficients and implications for diffusion studies with compacted clays. *Clay Clay Miner.* 56, 677–685.
- Glaus, M.A., Aertsens, M., Maes, N., Van Laer, L., Van Loon, L.R., 2015. Treatment of boundary conditions in through-diffusion: a case study of Sr-85⁽²⁺⁾ diffusion in compacted illite. *J. Contam. Hydrol.* 177, 239–248.
- Glaus, M.A., Van Loon, L.R., Wüst, R.A.J., 2023. Diffusion of HTO, ^{36}Cl and ^{22}Na in the Mesozoic rocks of northern Switzerland. II: Interpretation in terms of an electrical double layer model. *Appl. Geochem.*, 105842. <https://doi.org/10.1016/j.apgeochem.2023.105842>.
- Kiczka, M., Wersin, P., Mazurek, M., Zwahlen, C., Jenni, A., Mäder, U., Traber, D., 2023. Porewater composition in clay rocks explored by advective displacement and squeezing experiments. *Appl. Geochem.* 105838. <https://doi.org/10.1016/j.apgeochem.2023.105838>.
- Maes, N., Glaus, M., Baeyens, B., Marques Fernandes, M., Churakov, S., Dähn, R., Grangeon, S., Tournassat, C., Geckeis, H., Charlet, L., Brandt, F., Poonoosamy, J., Hoving, A., Havlova, V., Fischer, C., Scheinost, A., Noseck, U., Britz, S., Siitari-Kauppi, M., Missana, T., 2021. State-of-the-Art Report on the Understanding of Radionuclide Retention and Transport in Clay and Crystalline Rocks. Final Version as of 30.04.2021 of Deliverable D5.1 of the HORIZON 2020 Project EURAD. EC Grant agreement no, 847593.
- Mazurek, M., Gimmi, T., Zwahlen, C., Aschwanden, L., Gaucher, E.C., Kiczka, M., Rufer, D., Wersin, P., Marques Fernandes, M., Glaus, M., Van Loon, L., Traber, D., Schnellmann, M., Vietor, T., 2023. Swiss deep drilling campaign 2019–2022: Geological overview and rock properties with focus on porosity and pore-space architecture. *Appl. Geochem.* 105839. <https://doi.org/10.1016/j.apgeochem.2023.105839>.
- NEA, 2013. The Nature and Purpose of the Post-closure Safety Case For Geological Repositories. NEA/RWM/R. OECD/NEA, Paris (2013)1.
- Shackelford, C.D., Moore, S.M., 2013. Fickian diffusion of radionuclides for engineered containment barriers: diffusion coefficients, porosities, and complicating issues. *Eng. Geol.* 152, 133–147.
- Takeda, M., Nakajima, H., Zhang, M., Hiratsuka, T., 2008a. Laboratory longitudinal diffusion tests: 1. Dimensionless formulations and validity of simplified solutions. *J. Contam. Hydrol.* 97, 117–134.
- Takeda, M., Zhang, M., Nakajima, H., Hiratsuka, T., 2008b. Laboratory longitudinal diffusion tests: 2. Parameter estimation by inverse analysis. *J. Contam. Hydrol.* 97, 100–116.
- Van Laer, L., Aertsens, M., Maes, N., Glaus, M., Van Loon, L., 2022. Diffusion Experiments on Clayey Rock Samples from Nagra's Deep Drilling Campaign as Part of a Benchmarking Study. In: *Arbeitsbericht NAB*, vols. 22–23. NAGRA, Wettingen, Switzerland. <https://nagra.ch/downloads/arbeitsbericht-nab-22-23/>.
- Van Loon, L.R., Soler, J.M., 2003. Diffusion of HTO, $^{36}\text{Cl}^-$, $^{129}\text{I}^-$ and $^{22}\text{Na}^+$ in Opalinus Clay: Effect of Confining Pressure, Sample Orientation, Sample Depth and Temperature. PSI Bericht 04-03. Paul Scherrer Institute, Villigen, Switzerland. Also published as Nagra Technical Report NTB 03-07, Nagra, Wettingen, Switzerland. <https://nagra.ch/en/downloads/technical-report-ntb-03-07-2/>.
- Van Loon, L.R., Muller, W., Iijima, K., 2005. Activation energies of the self-diffusion of HTO, $^{22}\text{Na}^+$ and $^{36}\text{Cl}^-$ in a highly compacted argillaceous rock (Opalinus Clay). *Appl. Geochem.* 20, 961–972.
- Van Loon, L.R., 2014. Effective Diffusion Coefficients and Porosity Values for Argillaceous Rocks and Bentonite: Measured and Estimated Values for the Provisional Safety Analyses for SGT-E2. Nagra Technical Report NTB 12-03, Nagra, Wettingen, Switzerland. <https://nagra.ch/en/downloads/technical-report-ntb-12-03-2/>.

Van Loon, L.R., Leupin, O.X., Cloet, V., 2018. The diffusion of SO_4^{2-} in Opalinus Clay: measurements of effective diffusion coefficients and evaluation of their importance in view of microbial mediated reactions in the near field of radioactive waste repositories. *Appl. Geochem.* 95, 19–24.

Van Loon, L.R., Bunic, P., Frick, S., Glaus, M.A., Wüst, R.A.J., 2023. Diffusion of HTO, ^{36}Cl and ^{22}Na in the Mesozoic rocks of Northern Switzerland. I: Effective diffusion

coefficients and capacity factors across the heterogeneous sediment sequence. *Appl. Geochem.* 105843. <https://doi.org/10.1016/j.apgeochem.2023.105843>.
Zwahlen, C., Gimmi, T., Jenni, A., Kiczka, M., Mazurek, M., Van Loon, L., Mäder, U., Traber, D., 2023. Chloride accessible porosity fractions across the Jurassic sedimentary rocks of Northern Switzerland. *Appl. Geochem.* 105841. <https://doi.org/10.1016/j.apgeochem.2023.105841>.